ISSN 1027-5495. Functional Materials, 33, No.3 (2026), p. 517-525
doi:http://dx.doi.org/10.15407/fm33.03.517 © 2026 — SSI "Institute for Single Crystals"
This is an open access article under the CC BY-NC-ND license (http://creativecommons.org/licenses/by-nc-nd/4.0/).

Apatite-containing glass-ceramic matrices for immobilization of radioactive waste

O. Savvova[1], M. Hozha[1], Ye. Svitlychnyi[2], O. Babich[1], M. Tymoshchuk[1], O. Khrystych[1], T. Shkolnikova[3]

[1]O.M. Beketov National University of Urban Economy in Kharkiv, 17, Chornoglazivska Street, Kharkiv, 61002, Ukraine
[2]National Scientific Center Kharkiv Institute of Physics and Technology 1, Akademichna St., Kharkiv, 61108, Ukraine
[3]Department of General and inorganic chemistry, National Technical University «Kharkiv Polytechnic Institute» 2, Kyrpychova Str., 61000, Kharkiv, Ukraine
corresponding author e-mail:

Received January 15, 2026, approved March 25, 2026

The article analyzes the advantages of using glass-ceramic materials for immobilizing low- and medium-level radioactive waste, which have high operational characteristics, availability of raw materials, and environmental friendliness of the technology. Requirements for the properties of solid matrices and the characteristics of glassy-ceramic materials compositions for immobilizing radioactive waste were determined. A composition of glass-ceramic material based on the SiO_2–Al_2O_3–B_2O_3–CaO–P_2O_5–TiO_2–ZrO_2–CeO_2–ZnO–BaO–MoO_2 system in the region of hydroxyapatite crystallization has been developed. It has been established that the mechanism of phase formation in glass consists of the formation of a dissipative crystalline structure of glass-ceramic materials during low-temperature heat treatment. The composition of the material was modified by introducing cesium and strontium salts, and the efficiency of their incorporation into the glassy-ceramic materials structure under thermal treatment was determined. Simulation experiments were carried out to study the retention of these elements in the material structure. The developed high-strength glass-ceramic material is characterized by a fine-dispersed structure and a hydroxyapatite content of 50 vol.%. This material can retain approximately 80-95% of cesium and strontium elements in its structure, which determines the prospects for using the proposed material as a solid matrix for immobilizing radioactive waste.

Keywords: glass-ceramic materials, immobilization, radioactive waste, structure, crystallization, hydroxyapatite, strength, radiation safety.

Апатитовмісні склокерамічні матриці для іммобілізації радіоактивних відходів.
О. Саввова, М. Гожа, Є. Світличний, О. Бабіч, М. Тимощук, О. Христич, Т.Школьнікова

У статті проаналізовано переваги використання склокерамічних матеріалів для іммобілізації низько- та середньоактивних радіоактивних відходів. Ці матеріали відрізняються високими експлуатаційними характеристиками, доступністю сировини та екологічністю технології. Визначено вимоги до властивостей твердих матриць та характеристики складів склокерамічних матеріалів для іммобілізації радіоактивних відходів. Розроблено склад склокерамічного матеріалу на основі системи SiO_2–Al_2O_3–B_2O_3–CaO–P_2O_5–TiO_2–ZrO_2–CeO_2–ZnO–BaO–MoO_2 в області кристалізації гідроксиапатиту. Встановлено, що механізм фазоутворення у склі полягає у формуванні дисипативної кристалічної структури склокерамічних матеріалів під час низькотемпературної термічної обробки. Склад матеріалу було модифіковано шляхом введення солей цезію та стронцію, а також визначено ефективність

їх включення в структуру склокерамічних матеріалів при термічній обробці. Були проведені моделювальні експерименти для дослідження утримання цих елементів у структурі матеріалу. Розроблений високоміцний склокерамічний матеріал характеризується дрібнодисперсною структурою та вмістом гідроксиапатиту 50 об.%. Цей матеріал може утримувати у структурі приблизно 80-95% елементів цезію та стронцію, що визначає перспективи використання запропонованого матеріалу як твердої матриці для іммобілізації радіоактивних відходів.

1. Introduction

Currently, the assurance of radiation safety constitutes a key prerequisite for creating living conditions in accordance with the effective international radiation safety standards and regulations.

The main technologies for radioactive waste (RAW) immobilization that are commercially available and have demonstrated their viability are cementation, bituminization, and vitrification [1, 2]. The advantages of vitrification lie in the high capacity of borosilicate or phosphate glasses to incorporate elements regardless of their charge and atomic size, high chemical stability, radiation resistance, and the ability to avoid phase separation and uncontrolled crystallization, which weakens glass structure. The incorporation of waste into glass matrices has proven effective and corresponds to TRL 7–9 [3,4]. An additional advantage of this waste immobilization technology is the reduction of its volume and, consequently, the reduction of the waste disposal area.

A significant challenge in vitrification technology for RAW immobilization is the relatively low mechanical strength of glasses, which affects their ability to resist brittle fracture and absorb or dissipate acoustic waves. Ensuring high mechanical strength is particularly important when glasses are used in areas with increased seismic activity. The Fukushima-1 accident, which resulted in releases of radioactive cesium and iodine, demonstrated the necessity of such properties [5].

Due to the risks associated with numerous hazards, the presence and operation of nuclear facilities must comply with clear regulatory standards: ASCE/SEI 4-2016 [6], ANSI/ANS-2.26-2004 (R2021), ANSI/ANS- 2.27-2020 (R2025), ANSI/ANS- 2.29-2020 (R2025) [7]. The escalation of armed conflicts and the increasing destructive potential of explosive weapons lead to damage to nuclear power plants: nuclear reactors, cooling and safety systems, turbines, generators, as well as storage and processing systems for spent nuclear fuel and RAW [8].

The solution to this urgent problem is the creation of high-tech functional glass-ceramic materials (GCMs), which are characterized by:

– technological efficiency (availability of raw materials, reduced synthesis temperatures, and reproducibility of technological processes;

– high performance properties (thermal stability, high mechanical strength, chemical and radiation resistance);

– reduced cost due to the exclusion of expensive raw components from glass composition and the use of accessible raw materials;

– environmental friendliness of the technology by excluding potentially hazardous raw components and minimizing emissions in the technological process.

The choice of glass-ceramic materials (GCMs) is based on their indisputable advantages over purely glassy and crystalline materials, which have been implemented in many countries, including Australia, France, Japan and the USA [9].-

The most common crystalline phases in GCMs include zirconolite, pyrochlore, and britolite in borosilicate glass, as well as monazite or NZP in phosphate systems. Known high-strength multifunctional glass-ceramic materials contain crystalline phases such as lithium disilicate ($Li_2Si_2O_5$) [10, 11], spodumene $LiAlSi_4O_{10}$) [10, 12], willemite [13], cordierite [14], among others. However, lithium-containing GCMs are relatively expensive, while magnesium aluminosilicate GCMs require high synthesis temperatures and are characterized by significant viscosity. Moreover, the fracture toughness values of GCMs rarely exceed 3.5–4.0 MPa $\cdot m^{0.5}$, which limits their use under significant dynamic loads, and their high cost restricts their application in large-scale processes such as RAW immobilization.

Recently, in the development of functional glass-ceramic materials, along with borosilicate and phosphate glasses [15, 16], apatite-containing materials are promising; they are used as bone substitutes in orthopedics and dentistry, phosphors for fluorescent lamps, laser receivers, gas sensors, and catalytic

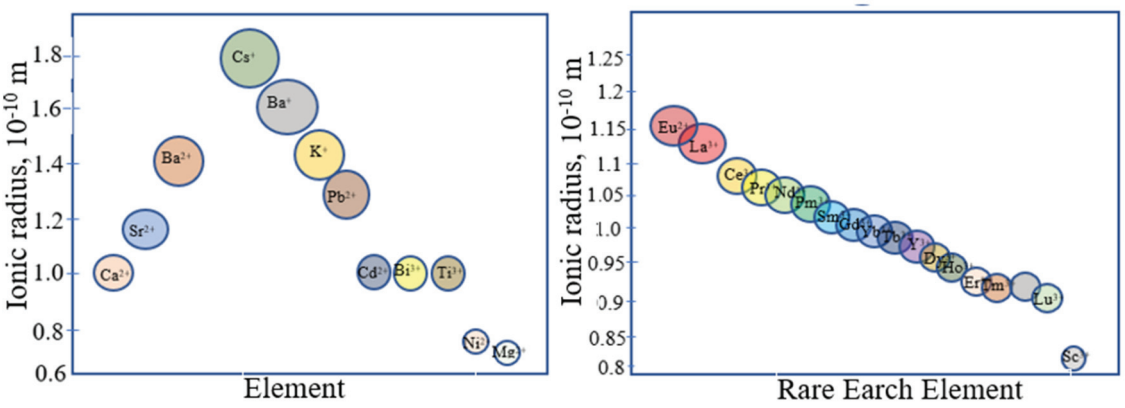

Figure 1 – Ionic radii of elements that can be accommodated instead of M in the lattice of apatite ($M_{10}(XO_4)_3Z_2$) [18]

materials [17]. Their ability to undergo isomorphic substitution of cations and anions, according to biomimetic principles of Earth minerals, enables effective immobilization of heavy metals (Zn, Mn, Pb, Cd) in situ in contaminated sediments, thereby significantly reducing anthropogenic environmental impact [15]. It is known [18] that more than half of the natural elements can be placed in the apatite matrix. The high thermal stability of hydroxyapatite (HAp) is due to a combination of crystallochemical and thermodynamic factors: a strong ionic-covalent crystal lattice, a high lattice energy, thermodynamic stability of the phosphate phase, and a wide range of isomorphic substitutions without lattice destruction.

The following substitutions have been identified in the structure of apatite ($M_{10}(XO_4)_6Z_2$) (Fig. 1):

The synthesis conditions (method, composition, temperature) determine the specific features of element substitution in apatites, in particular within the phosphorus–silicate structure of lanthanide–strontium compounds [19]. The results obtained by the authors [20] indicate the promising potential of using nanoparticles of complex-substituted calcium phosphates for the immobilization of cesium in stable crystalline materials of the whitlockite or apatite type.

Therefore, the development and implementation of high-strength apatite-containing glass-ceramic materials for the immobilization of radioactive waste is of considerable scientific and practical importance.

2. Experimental

2.1. Requirements for the properties of solid-state matrices and features of glass-ceramic compositions for the immobilization of radioactive waste

For the production of high-strength glass-ceramic materials of this type, calcium–silicophosphate glasses were selected, allowing for the crystallization of hydroxyapatite crystals [21] through a phase separation mechanism enabled by the simultaneous presence of silicon, phosphorus, and zinc oxides. The selected glass compositions were modified with oxides that exhibit a synergistic effect in forming their structure and ensuring properties. The modification of apatite-containing glass compositions was carried out taking into account the authors' previous studies [21– 26]. The following tasks were set:

– to ensure high thermal and chemical stability using oxides of aluminum, boron, zirconium, zinc, titanium;

– to ensure high radiation stability using oxides of cerium, barium, molybdenum, titanium;

– to reduce the melting point of glass: oxides of boron, zinc, and barium.

– to shift the nucleation region to the low-temperature region: oxides of cerium and zinc;

– to intensify the crystallization process for the formation of a sintered structure: oxides of zirconium and titanium.

2.2 Research methods

For the development of GSM, the composition of the experimental glass ASR-3M was selected with the following wt. %: SiO_2 – 45; ΣAl_2O_3, B_2O_3–20; ΣCaO, P_2O_5 – 20; TiO_2, ZrO_2,

CeO_2 – 7, ΣZnO, BaO – 7; MoO_2– 1. To prepare the batch for the synthesis of glass, natural mineral raw materials (Novoselivsky sand, alumina, zircon, chalk), oxides marked C.P. (chemically pure) (ZnO, TiO_2, MoO_2, CeO_2) and other chemical compounds (boric acid, barium carbonate, disubstituted ammonium phosphate) were used. The glasses were synthesized at a melting temperature of 1450 °C in corundum crucibles using an electric furnace equipped with molybdenum disilicide heating elements, followed by gradual cooling inside the furnace for 12 hours.

To obtain the compositions, powders of experimental glass and various types of cesium and strontium salts, as well as their mixtures, were used in an amount of 1.3–3.0 wt. % per 100 wt. % of glass. The types and contents of the salts were selected taking into account the data on the radionuclide composition of the salt cake, as a determining factor in the development of a liquid radioactive waste conditioning system [27]. To establish the possibility of incorporating radioactive isotopes of cesium and strontium, a simulation of this process was carried out by adding Cs_2SO_4, CsCl, and $SrCl_2 \cdot 6H_2O$ salts to the glass powder compositions (Table 1), followed by their thermal treatment up to 900 °C.)

The preparation of glass composites was carried out as follows:

1. The ACR-3M glass sample was ground to a residue of no more than 5% on a No. 008 sieve.

2. Glass composite samples based on ACR-3M and a specified amount of salts or their mixtures (Table 1) were prepared by semi-dry isostatic pressing (P = 35–40 MPa). They were formed into cylinders with a diameter of 4 mm and a height of 10 mm, using a xanthan gum solution (4 wt. %) as a temporary binder.

3. The samples were dried at a temperature of 120 °C for 1 hour.

4. The samples underwent heat treatment at a temperature of T = 850 °C (for 2 hours).

The glass composites based on glass and salts or their mixtures were subjected to heat treatment in a single-stage mode, taking into account the possibility of forming a finely dispersed structure containing hydroxyapatite and incorporating cesium and strontium cations into the structure.

It should be noted that salt melts obtained at deep evaporation plants of nuclear power plants with WWPR (Water-Water Power Reactor) reactors have a solid aggregate state (crystal hydrates) and their classification as liquid radioactive waste leads to numerous problems in the handling of such waste [28].

X-ray diffraction studies were carried out using a DRON-UM1 X-ray diffractometer with Cu-Kα radiation and a Ni selective absorption filter. The diffracted radiation was recorded with a scintillation detector. Phase identification (qualitative phase analysis) was performed using the COD crystallographic database. Quantitative phase analysis and determination of structural parameters of the identified phases were conducted by the Rietveld method (MAUD software). It should be noted that, in some cases, individual lattice parameters of certain phases were not refined (were fixed) due to the low symmetry of the phases and their minor content in the sample. For samples containing both crystalline and amorphous phases, the degree of crystallinity (approximately equal to the volume fraction of the crystalline phase) was calculated according to the formula:

$$X_c = I_c/(I_c+I_a)\cdot 100\%$$

where X_c is the degree of crystallinity;

I_c is the total integrated intensity of diffraction peaks;

I_a is the integrated intensity of the diffraction halo.

Differential scanning calorimetry and thermogravimetric analysis of the samples were performed using a simultaneous DSC-TGA thermal analyzer (TA Instruments SDT Q 600) in the temperature range of 25 to 1200 °C in corundum crucibles at a heating rate of 10 °C/min. Petrographic analysis of glass materials was performed using transparent sections on a NU–2e optical microscope (magnification from 25 to 1200 times) in transmitted light.

The elemental composition of glass-ceramic materials after drying and after heat treatment (Table 2) was determined using energy-dispersive X-ray fluorescence (EDXRF) spectrometers (Rigaku).

The stress intensity coefficient of materials (MPa $\cdot m^{1/2}$) was determined according to the calculation method based on measuring the hardness of samples using PMT-3. Compressive strength (MPa) was measured in accordance with EN 1748-2-1-2016, and the modulus of elasticity (GPa) was determined using the acoustic resonance method.

3. Results and discussion

The XRD study of the phase composition of glass-ceramic materials ACR-3M after heat

Table 1 – Composition of glass-ceramic-based ACR-3M

Experimental sample	Nature of heat treatment	Type, content and ratio of additives		
		Salt	Ratio	Content, wt.%
ACR-3M 1.1	after drying	Cs_2SO_4	–	1.3
ACR-3M 1.2	after firing	Cs_2SO_4	–	1.3
ACR-3M 2.1	after drying	CsCl	–	1.3
ACR-3M 2.2	after firing	CsCl	–	1,3
ACR-3M 3.1	after drying	$SrCl_2 \cdot 6H_2O$	–	1.3
ACR-3M 3.2	after firing	$SrCl_2 \cdot 6H_2O$	–	1.3
ACR-3M 4.1	after drying	Cs_2SO_4+$SrCl_2 \cdot 6H_2O$	1:1	1.5
ACR-3M 4.2	after firing	Cs_2SO_4 +$SrCl_2 \cdot 6H_2O$	1:1	1.5
ACR-3M 5.1	after drying	Cs_2SO_4 +$SrCl_2 \cdot 6H_2O$	1:1	2.6
ACR-3M 5.2	after firing	Cs_2SO_4+ $SrCl_2 \cdot 6H_2O$	1:1	2.6
ACR-3M 6.1	after drying	Cs_2SO_4 +$SrCl_2 \cdot 6H_2O$	1:1	3.0
ACR-3M 6.2	after firing	Cs_2SO_{4+} $SrCl_2 \cdot 6H_2O$	1:1	3.0
ACR-3M 7.1	after drying	CsCl +$SrCl_2 \cdot 6H_2O$	1:1	3.0
ACR-3M 7.2	after firing	CsCl +$SrCl_2 \cdot 6H_2O$	1:1	3.0

treatment (HT) (Fig. 2) revealed the presence of hydroxyapatite (lattice parameters a = 9.381; c = 6.889) and ß-$Ca_3(PO_4)_2$ (lattice parameters a = 10.336; c = 37.403) with a total content of 50 vol.%.

The presence of hydroxyapatite in the composition of glass-ceramic materials ensures the conditions for immobilization of strontium and cesium cations within the glassy phase and hydroxyapatite structure via isomorphic substitution. The presence of strontium-substituted HAP in the GCM ASR-3M3.1 composite is evidenced by a change in the parameters of the hydroxyapatite lattice a = 9.937; c = 6.875.

An important condition for the stabilization of embedded strontium and cesium cations is the formation of a fine-crystalline structure of the material, characterized by high strength and durability after low-temperature heat treatment. The formation of a finely dispersed structure is confirmed by the presence of hydroxyapatite crystals <0.5 µm, uniformly distributed within the glass matrix along distinct parallel bands in the crystallization front direction. This structural self-organization of glass indicates a mechanism of bulk crystallization through phase separation, which is characterized by the formation of nanoscale inhomogeneities in the range of nucleation temperatures (T = 700 °C) and their subsequent growth in the crystallization temperature region.

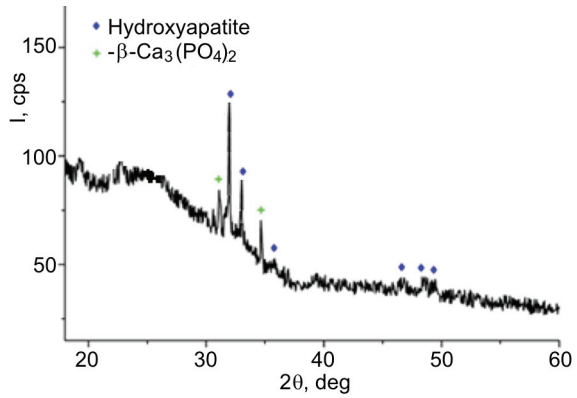

Figure 2 – X-ray diffraction pattern of experimental glass-ceramic materials ACR-3M

A characteristic feature of phase separation in the experimental glass ACR-3M is the presence of spherical (globular) phases dispersed within the residual glass matrix (Fig. 3a, I). The phase separation through the spinodal mechanism leads to the formation of interconnected phases of similar chemical composition (Fig. 3a, II), separated by diffuse interphase boundaries [29]. The appearance of a large number of glass crystal nuclei at the interfaces of spherical inhomogeneities by this mechanism is an energetically favorable process for forming a fine-crystalline structure of GCM at 850 °C. This structure is characterized by a high degree of ordering of structural units (crystals) 0.5–1 µm in size, self-organized into

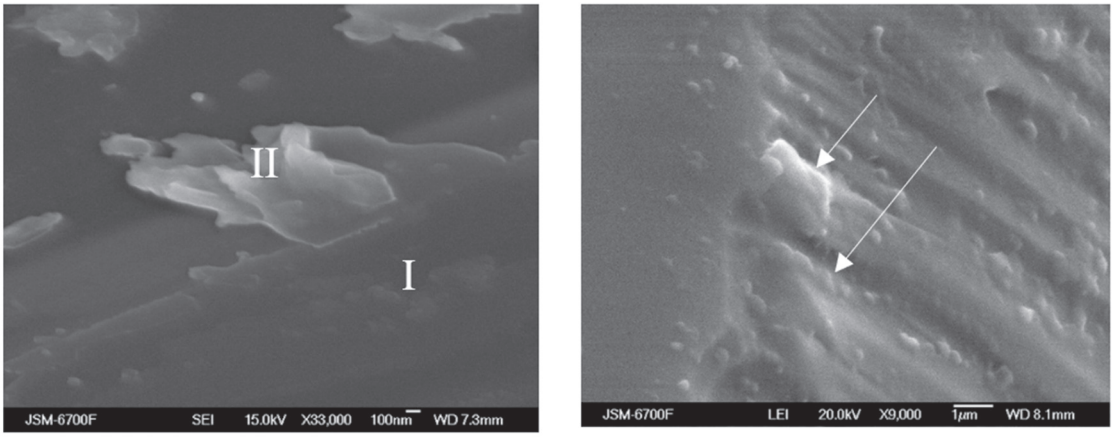

Figure 3 – Microphotographs of structure of ACR-3M sample after heat treatment at different temperatures: (a) T =700°C, (b) T=850 °C

distinct parallel conglomerates in the crystallization front direction (Fig. 3b). At the same time, structural formation of glasses in the low-temperature range (up to 850 °C) enables conditions for the inclusion of salts of radioactive isotopes contained in radioactive waste by reducing their volatilization.

A decrease in nucleation temperatures ensures the appearance of dissipative structures in the nonequilibrium steady state of silicate glass, which is structurally equilibrated under variable conditions with extremely long relaxation times. This relaxation process signifies the formation of negative entropy in the ideal glass as a result of local crystallization of molecules within the equilibrated amorphous glass phase [30].

The presence of a self-organizing dissipative structure in glass, capable of maintaining an ordered state under changing critical loads of temperature and stress, is an important criterion that ensures its strength and reliable immobilization of radioactive isotopes. The use of such self-organizing glass-ceramic materials is effective in the design of structures subject to destruction under the influence of simultaneous significant dynamic, thermal, chemical and biological loads [31]. .

The mechanical properties of ASR3M are sufficiently high due to the formation of a high-strength glass-ceramic structure. The relatively high fracture toughness value (3.3 MPa $\cdot m^{1/2}$) deserves special attention. Along with high values of elastic modulus (200 GPa) and compressive strength (140 MPa) compared to phosphate glasses and apatite ceramics, it will ensure the high viability of the material under significant dynamic impact.

Determination of the content of cesium and strontium elements, simulating the composition of the salt cake after their inclusion into the ACR-3M sample after drying and after heat treatment (Table 2), allowed for establishing the characteristics of their retention in the glass matrix. The change in the contents of Cs and Sr elements after firing ranges from 5.2 to 18 % and depends on the type and composition of the components. It was established that with the addition of cesium chloride in an amount of 1.3 wt. % per 100 wt. % of glass, the decrease in the cesium element content after heat treatment in the ACR-3M 2 sample is the highest and amounts to 18 %, which is due to the lowest melting point of CsCl among the tested salts ($T_{melting}$ = 645 °C). When adding cesium sulfate ($T_{melting}$ = 1019 °C) into the ACR-3M composition, this indicator slightly decreases and amounts to 13 % (sample 1). The addition of strontium chloride ($T_{melting}$ = 874 °C) reduces the strontium content to 11.6% for sample ACR-3M 3, indicating the possible incorporation of strontium cation into the hydroxyapatite structure during heat treatment.

With the simultaneous introduction of cesium sulfate and strontium chloride salts in an amount of 1.5 wt. % per 100 wt. % (ACR-3M 4) and 2.6 wt. % per 100 wt. % (ACR-3M 5), the total changes in the element content are 13.5% and 12.2%, respectively. This can be explained by the substitution of calcium in the HAp structure not only by strontium but also by cesium. With an increase in the content of cesium sulfate and strontium chloride salts to 3.0 wt. %

Table 2 – Changes in element content in the sample compositions

Experimental sample	Nature of heat treatment	Content (wt. %) and change in element content (%) in the composition of the samples			
		Content, wt.%	Change in element content after HT, %	Content, wt.%	Change in element content after HT , %
		Cs		Sr	
ACR-3M 1.1	after drying	0.96	13.0	–	–
ACR-3M 1.2	after firing	0.74		–	
ACR-3M 2.1	after drying	1.03	18.0	–	–
ACR-3M 2.2	after firing	0.82		–	
ACR-3M 3.1	after drying	–	–	0.43	11.6
ACR-3M 3.2	after firing	–		0.38	
ACR-3M 4.1	after drying	0.55	5.5	0.25	8.0
ACR-3M 4.2	after firing	0.52		0.23	
ACR-3M 5.1	after drying	0.96	5.2	0.43	7.0
ACR-3M 5.2	after firing	0.91		0.40	
ACR-3M 6.1	after drying	1.0	8.0	0.43	7.0
ACR-3M 6.2	after firing	0.92		0.40	
ACR-3M 7.1	after drying	1.10	11.3	0.50	9.0
ACR-3M 7.2	after firing	0.91		0.45	

per 100 wt. % (ACR-3M 6), the content of the strontium element in the structure does not change, while the content of the cesium element slightly increases, amounting to 8 % overall.

With the simultaneous introduction of cesium and strontium chloride salts into the ACR-3M composition, the total change in the element content is 20.3% (ACR-3M 7), showing a higher intensity for the cesium element. Based on the obtained results, it can be concluded that the ACR-3M apatite-containing glass material is promising as a matrix for radioactive waste immobilization. Changes in the content of cesium and strontium elements after heat treatment do occur, but in the general case, they are insignificant the framework of the experiment.

Along with the ability of glass structures to retain Cs^+ and Sr^{2+} cations for their immobilization in the crystalline and glassy phases, an important factor facilitating their incorporation is the reduction in the formation temperature of GCM structure based on ACR-3M compared to the formation temperature (○> 1000 °C) of glass-ceramic matrices for radioactive waste immobilization [32]. Thus, the low temperature of structure formation of the experimental samples with vitrification of the glass phase at 900 °C, which is below the boiling points of $SrCl_2$, CsCl, and Cs_2SO_4 ($T_{boiling}$ = 1300, 1290, and 1900 °C, respectively), ensures their stability in the GCM structure during heat treatment.

The results of thermal analysis allowed for determining the mass loss changes in both the initial ACR-3M sample and the initial ACR-3M 7.1 mixture. On the TGA curves of both materials, which are virtually identical, minor mass losses are observed as the temperature increases up to 900 °C (Fig. 4). The DSC curves exhibited a low-temperature endothermic effect (50–200 °C), attributed to the removal of adsorbed water, and stress relaxation (200–300 °C). A broad, combined exothermic effect observed on the DSC curves of the GCMs indicated the occurrence of solid-phase reactions (300–400 °C) and glass formation (400–500 °C), followed by softening (700–800 °C) and vitrification (900–1100 °C).

Changes in sample behavior were recorded on the TGA curves starting from 900 °C, when significant mass losses were observed. In the initial ACR-3M sample, the high melting temperature was due to the presence of hydroxyapatite, which melts at 1100 °C. The reduced mass loss observed for the ACR-3M 7.1 sample was associated with the formation of solid solutions by isomorphic substitution of Cs^+ and Sr^{2+} ions in the hydroxyapatite structure and

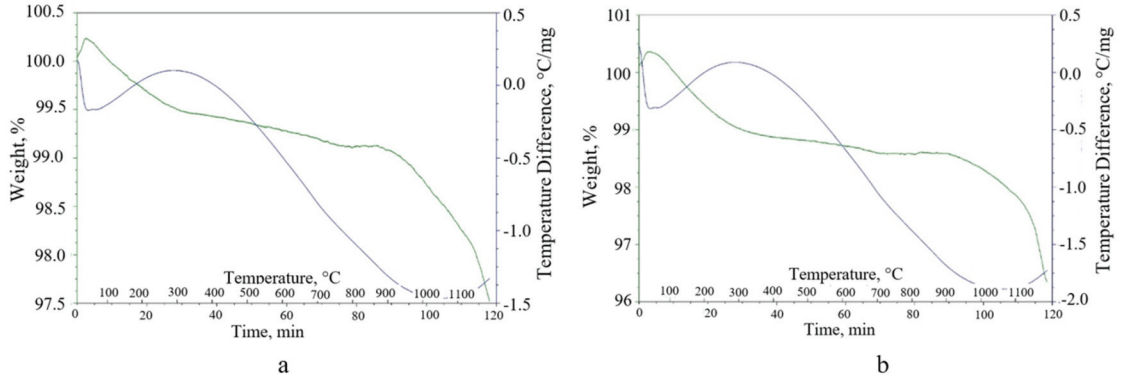

Figure 4 – Differential scanning calorimetry (DSC) and thermogravimetric analysis (TGA) of the initial ACR-3M sample and the initial ACP3-M 7.1 mixture: a – ACR-3M; b – ACR-3M 7.1

the corresponding shift in the melting range towards temperatures above 1100 °C (Fig. 4).

A comparative analysis of the developed apatite-containing glass-ceramic material with known matrices for radioactive waste immobilization demonstrated its significant advantages. Unlike solid-state matrices based on phosphate glasses [33], which are characterized by synthesis temperatures of 850–1050 °C and limited mechanical properties, as well as calcium phosphate ceramic matrices formed at 750–800 °C [34] but possessing insufficient strength for operation under significant mechanical loads, the developed material forms a finely dispersed glass-ceramic structure already at a temperature of 850 °C. It is characterized by a high fracture toughness value (3.3 MPa·$m^{1/2}$) compared to phosphate glasses and apatite ceramics, which, along with high values of elastic modulus (200 GPa) and compressive strength (140 MPa), will ensure high performance characteristics of the material.

Compared to glass-ceramic matrices based on $NaZr_2(PO_4)_3$ [32], which are characterized by high chemical stability but require higher synthesis temperatures, the proposed material combines low-temperature structure formation with high radioactive component retention efficiency. The presence of about 50 vol.% of hydroxyapatite in the structure creates favorable conditions for the isomorphous incorporation of strontium and cesium cations into the crystalline phase. According to the research results, it was established that after thermal treatment, 80–95% of the introduced strontium and cesium elements are retained within the structure of the glass-ceramic material, which demonstrates its promise for use as a solid-state matrix for radioactive waste immobilization.

4. Conclusions

A composition of a calcium–phosphate–silicate glass, modified with oxides of aluminum, boron, zirconium, zinc, cerium, barium, molybdenum, and titanium, was substantiated and developed. These modifiers promote the formation of a glass–ceramic structure at relatively low temperatures. The mechanism of phase formation in the glass structure was investigated, and it was found that the ordered dissipative glass–ceramic structure of the material is formed through the spinodal phase separation mechanism at a hydroxyapatite content of about 50 vol.%.

Studies of the inclusion of cesium and strontium, simulating the composition of the salt melt, after their introduction into ACR-3M sample followed by drying and heat treatment, showed that the addition of Cs_2SO_4, CsCl, and $SrCl_2 \cdot 6H_2O$ salts in amounts of 1.3–3.0 wt.% per 100 wt.% of glass allows immobilization of 80–95 wt.% of Cs^+ and Sr^{2+} cations within the of the apatite-containing glass-ceramic material structure.

The developed apatite-containing glass-ceramic material is a promising solid-state matrix for RAW immobilization, which stands out among traditional analogues due to its high competitiveness achieved through its excellent ability for structural self-organization, allowing the retention of cesium and strontium cations within the structure at low structure formation temperatures.

References

1. M.L. Ferreira Nascimento, D.R. Cassar, R. Ciolini et al., Infrastructures, 7(9), 120 (2022). https://doi.org/10.3390/infrastructures7090120.

2. M.I. Ojovan and S.V. Yudintsev, Open Ceram. 14, 100355 (2023). https://doi.org/10.1016/j.oceram.2023.100355
3. O. Savvova, Y. Pokroieva, I. Luhovoi et al., IOP Conf. Ser.: Earth Environ. Sci. 1376, 012025 (2024). https://doi.org/10.1088/1755-1315/1376/1/012025
4. O. Savvova, M. Hozha, I. Zaitseva, et al., IOP Conf. Ser.: Earth Environ. Sci. 1499, 012065 (2025). https://doi.org/10.1088/1755-1315/1499/1/012065
5. R. Wakeford, J. Radiol. Prot. 41, E1 (2021). https://doi.org/10.1088/1361-6498/abecc2
6. J.S. McCloy and A. Goel, MRS Bulletin. 42(3), 233 (2017). https://doi.org/10.1557/mrs.2017.8
7. ANS - American Nuclear Society. ANS Catalog https://store.accuristech.com/ans/subgroups/55480?page=3&per_page=10
8. Y. Wang, IJSSPA, 5(2), 243 (2024). https://doi.org/10.62051/ijsspa.v5n2.30
9. M.B. Almendro-Candel and M.M. Jordán Vidal, Coatings., 14, 346 (2024). https://doi.org/10.3390/coatings14030346
10. Y. Hu, Y. Rao, M. Wang et al., Wuhan Univ. Technol.–Mater. Sci. Ed. 39, 551 (2024). https://doi.org/10.1007/s11595-024-2911-9
11. O. Savvova, G. Voronov, V. Topchyi et al., Chem. Chem. Technol. 12, 391 (2018). https://doi.org/10.23939/chcht12.03.391
12. O.V. Savvova, O.V. Babich, G.K. Voronov et al., Strength Mater. 49, 479 (2017). https://doi.org/10.1007/s11223-017-9890-4
13. S. Węgrzyk, D. Herman and M. Pancielejko, J. Non-Cryst. Solids 582, 121443 (2022). https://doi.org/10.1016/j.jnoncrysol.2022.121443
14. J.Y. Kim, S.W. Choi, K.S. Park et al., Ceram. Int. 50(19A), 35725 (2024). https://doi.org/10.1016/j.ceramint.2024.06.390
15. Y. Zhang, H. Zhang et al., Environ. Earth Sci. 78 (94) (2019). https://doi.org/10.1007/s12665-019-8085-7
16. S.Y. Sayenko, Y.O. Svitlychnyi, V.A. Shkuropatenko et al., Funct. Mater. 27(1), 39 (2019). https://doi.org/10.15407/fm27.01.39
17. T. Duminis, S. Shahid and R.G. Hill, Front. Mater. 3, 59 (2017). https://doi.org/10.3389/fmats.2016.00059
18. P. Ptacek, Advanced Methods and Applications in Material Science, IntechOpen (2016). https://doi.org/10.5772/62213
19. K. Kthiri, M. Mehnaoui, N. Ihzaz et al., Mater. Chem. Phys. 340, 130787 (2025). https://doi.org/10.1016/j.matchemphys.2025.130787
20. O. Livitska, N. Strutynska, K. Loza et al., Chem. Central J. 12, 87 (2018). https://doi.org/10.1186/s13065-018-0455-9
21. O.V. Savvova, V.M. Shimon, O.V. Babich et al., Funct. Mater. 27(4), 767 (2020). https://doi.org/10.15407/FM27.04.767
22. Z. Wang, X. Lin, X. Jiang, L. Liu et al., Ceram. Int. 49(11B), 19091 (2023). https://doi.org/10.1016/j.ceramint.2023.03.036
23. K. Dadwal, A. Khanna, P. Bhattacharya et al., J. Am. Ceram. Soc. 108(9) (2025). https://doi.org/10.1111/jace.20635
24. K. Won-in, N. Sirikulrat and P. Dararutana, Adv. Mater. Res. 214, 207 (2011). https://doi.org/10.4028/www.scientific.net/AMR.214.207
25. A.F. Abd El-Rehim, H.Y. Zahran, I.S. Yahia et al., Silicon 14, 405 (2022). https://doi.org/10.1007/s12633-020-00827-1
26. H. Shendy, G.A. Khater, M.G. Shahien et al., Constr. Build. Mater. 411, 134745 (2024). https://doi.org/10.1016/j.conbuildmat.2023.134745
27. V.G. Rudychev, N.A. Azarenkov, I.O. Girka et al., Probl. At. Sci. Technol. 5 (2019). http://dspace.nbuv.gov.ua/handle/123456789/195218
28. Yu.O. Olkhovyk, Nuclear energy and the environment, 2, 24 (2022). https://doi.org/10.31717/2311-8253.22.2.4 [in in Ukrainian]
29. S.A. Hassanzadeh-Tabrizi, J. Alloys Compd. 968, 171914 (2023). https://doi.org/10.1016/j.jallcom.2023.171914
30. S. Schuller, Atomic Energy and Alternative Energies Commission (2018). https://www.researchgate.net/publication/323692362
31. H. Kobayashi and H. Takahashi, Jpn. J. Appl. Phys. 60(4), 047002 (2021). https://doi.org/10.35848/1347-4065/abea53
32. J. Liu, F.Wang, Q. Liao et al., J. Nucl. Mater. 513, 251 (2019). https://doi.org/10.1016/j.jnucmat.2018.11.002
33. P. Stoch and M. Ciecinska, J. Therm. Anal. Calorim. 108, 705 (2012). https://doi.org/10.1007/s10973-011-1974-y
34. I.W. Donald, B.L. Metcalfe, S.K. Fong et al., J. Nucl. Mater, 361 (1), 78 (2007).https://doi.org/10.1016/j.jnucmat.2006.11.011